Critical condition for spectrum distortion of pump–probe-based stimulated Brillouin scattering in an optical fiber

Applied Physics Express 7, 082501 (2014)
http://dx.doi.org/10.7567/APEX.7.082501

Critical condition for spectrum distortion of pump–probe-based stimulated Brillouin scattering in an optical fiber

Xin Long, Weiwen Zou*, Hao Li, and Jianping Chen

State Key Laboratory of Advanced Optical Communication Systems and Networks, Department of Electronic Engineering, Shanghai Jiao Tong University, Shanghai 200240, China
E-mail: wzou@sjtu.edu.cn

Received June 25, 2014; accepted July 8, 2014; published online July 25, 2014

Spectrum distortion induced by pump depletion of pump–probe-based stimulated Brillouin scattering along an optical fiber is investigated theoretically and experimentally. Spectral hole burning is observed in the middle of the fiber. The critical condition for spectrum distortion is defined, and normalized parameters are introduced to describe the critical condition with different injected powers in arbitrary-length fibers. The experimental observation is in reasonable agreement with the numerical analysis. The different spectrum distortion may introduce novel applications to programmable optical fiber filtering. © 2014 The Japan Society of Applied Physics

Stimulated Brillouin scattering (SBS) is a nonlinear phenomenon that occurs through the generation of a backward Stokes wave whose frequency is downshifted from that of the pump laser.[1)] Since the basic SBS was first observed in an optical fiber,[2)] many fundamental SBS-related effects have been discovered[3–8)] and several applications[9–13)] have been developed. For example, spectrum broadening and hole burning, which were first observed in an SBS generator (i.e., noise-started spontaneous Brillouin scattering), have been explained as the result of the waveguide interaction, generated from different angular components of the pump and Stokes signals.[3)] During the application of an SBS-based amplifier, two coherent optical waves with a frequency difference equal to the Brillouin frequency shift are first launched into optical fibers; then, the frequency-scanned weak signal launched from the same end of Stokes wave could suffer non-uniform amplification if the two coherent waves' powers are too high.[4,5)] Furthermore, in SBS-based distributed fiber optical sensors,[9–12)] which have been regarded as powerful tools to monitor the structural health of smart materials and structures, two coherent waves [pulse and/or continuous wave (CW)] are injected into the two opposite ends of the sensing fiber. In comparison, time-domain distributed sensors are excellent for long sensing distances owing to their time-of-flight nature.[10–12)] Most recently, it has been found that pump depletion of a pump–probe-based configuration could induce a significant measurement error in the local Brillouin frequency shift at the far end of the probe (Stokes) wave.[11)] However, to the best of our knowledge, there are no reports on the effect of pump depletion inside an optical fiber that may distort the local Brillouin gain spectrum (BGS) based on pump–probe measurement configuration, which is important to evaluate the system performance of pump–probe-based SBS characterization and SBS-based distributed sensors.

In this work, we demonstrate a theoretical and experimental study of characterizing the spectrum distortion (including broadening, saturation, and hole burning) induced by pump depletion of the SBS in an optical fiber. BGS saturation is considered to be the critical condition that distinguishes these phenomena. Subsequently, we define the critical position and critical powers. We deduce the dimensionless coupling equations to describe the universal critical conditions with different configuration parameters (including injected powers, fiber length, and position). An experimental configuration is employed to characterize the BGS of the pump–probe-based configuration in the middle of the optical fiber. The experimental results agree well with the numerical simulations.

Assuming that a CW probe wave, $P_s(0)$, is injected at the near end of the fiber ($z = 0$) while a CW pump wave, $P_p(l)$, is launched at the far end of the fiber ($z = l$, where l is the fiber length), the coupling equations describing the pump–probe-based SBS interaction can be written as:[1)]

$$\begin{aligned} dP_p/dz &= GP_pP_s + \alpha P_p, \\ dP_s/dz &= GP_pP_s - \alpha P_s, \end{aligned} \tag{1}$$

where α is the fiber transmission loss and P_p (P_s) is the pump (probe) power at position z. $G = g/A_{eff}$ is the effective Brillouin gain, where A_{eff} is the effective area and $g = g_0 \cdot L(\nu)$, with g_0 the Brillouin gain coefficient and $L(\nu)$ the normalized Lorentz function of the pump–probe frequency difference (ν).

Through scanning ν in Eq. (1), we simulate the distribution of the BGS along the fiber for different l (= 50 m or 1 km) or $P_p(l)$ (= 20, 26, 0, or 10 dBm). The simulation results are depicted in Fig. 1. The parameters used are set as follows: $g_0/A_{eff} = 1\,(\mathrm{m{\cdot}W})^{-1}$, $P_s(0) = 0$ dBm, and Brillouin frequency shift $\nu_B = 10.85$ GHz at 1550 nm. There are different distortions of the BGS for different pump powers. For instance, when $l = 50$ m, the BGS along the fiber maintains the Lorentz shape for $P_p(l) = 20$ dBm [see Fig. 1(a)], while the BGS clearly broadens and spectral hole burning occurs in the middle of the fiber for $P_p(l) = 26$ dBm [see Fig. 1(b)]. As shown in Figs. 1(c) and 1(d), similar behavior is displayed for a longer fiber but lower power level.

Figure 2(a) illustrates the normalized BGS at different positions of Fig. 1 for a clear comparison. It is found that the BGS gradually becomes broadened, saturated, and hole burned when the position moves from the far end ($z = l$) towards the near end of the fiber ($z = 0$). Here, we define the BGS saturation as the critical condition of spectral hole burning phenomenon. For a given power level in an optical fiber, the critical condition determines a critical position that divides the fiber into two segments: no spectral hole burning takes place in the segment close to $z = l$; while it can occur anywhere in the segment close to $z = 0$.

In order to fully analyze the critical position for an arbitrary-length fiber and different injected pump or probe powers, we introduce the dimensionless equations, neglecting the transmission loss:

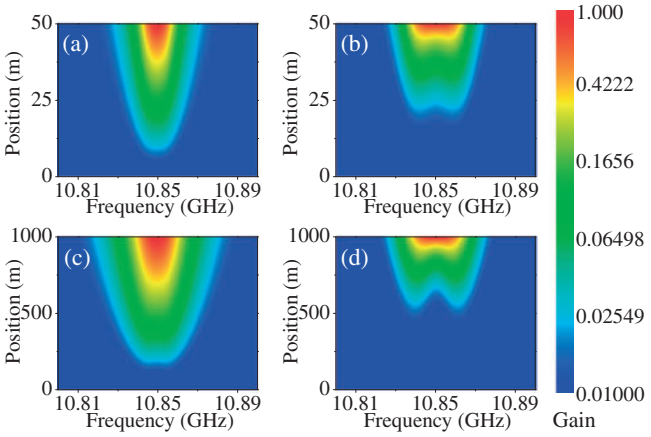

Fig. 1. Numerical simulation of the BGS distribution in an optical fiber. The fiber length is 50 m (a, b) or 1 km (c, d). The injected power is 0 dBm for probe waves and (a) 20, (b) 26, (c) 0, or (d) 10 dBm for pump waves. The effective Brillouin gain at the Brillouin frequency shift is set as $g_0/A_{\text{eff}} = 1\,(\text{m}\cdot\text{W})^{-1}$ and the transmission loss is neglected.

$$dQ_p/dx = kQ_pQ_s,$$
$$dQ_s/dx = kQ_pQ_s, \tag{2}$$

where $Q_p = P_p/P_s(0)$ and $Q_s = P_s/P_s(0)$ represent the normalized pump and probe waves, respectively, with respect to the injected probe wave $P_s(0)$, $x = z/l$ is the normalized position, and $k = G \cdot l \cdot P_s(0)$ is the normalized Brillouin gain.

We further introduce the injected power ratio between the pump and probe waves, which is defined as $\gamma = Q_p(x = 1) = P_p(l)/P_s(0)$. Considering $dQ_p/dx = dQ_s/dx$ in Eq. (2), i.e., the difference between Q_p and Q_s is maintained constant, we define $A = Q_p - Q_s$, which is determined by k and γ. Consequently, the analytical solutions to Eq. (2) can be derived as

$$Q_p = \frac{A(A+1)e^{-kAx}}{(A+1)e^{-kAx} - 1},$$
$$Q_s = \frac{A}{(A+1)e^{-kAx} - 1}. \tag{3}$$

The critical condition (i.e., BGS saturation, as defined above) of the spectral hole burning phenomenon can be theoretically expressed by:

$$\frac{dQ_s}{dv} = 0. \tag{4}$$

The above-mentioned critical position x_c can be evaluated by numerically solving Eqs. (4) and (3). Figure 2(b) depicts the calculated relation of x_c to k and γ, which indicates that x_c moves towards the fiber's far end when k and γ reach higher values (i.e., the fiber gets longer or the injected powers are stronger). This means that the pump depletion worsens, since much longer segments in the fiber suffer spectral hole burning.

In fact, the BGS at a fixed position varies with the change of either the pump or probe power, exactly as depicted in Fig. 2(a). Therefore, we further define the critical powers of the pump and probe waves to characterize the critical condition of the BGS saturation, beyond which the spectral hole burning phenomenon occurs at a specific position in a fiber, and vice versa. It must be noted that the physical nature

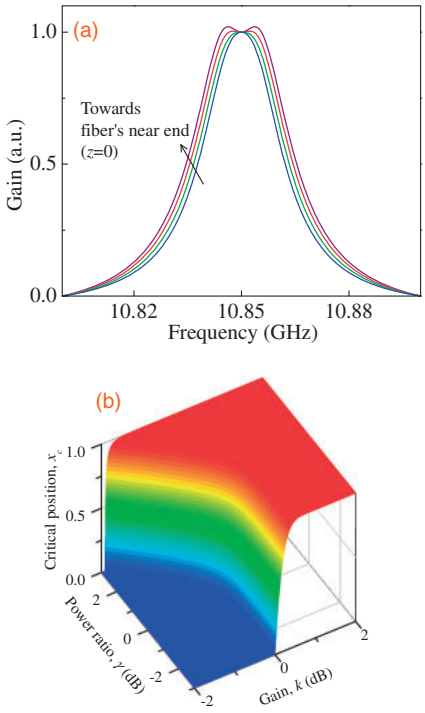

Fig. 2. (a) Comparison of normalized BGS at different positions in the fiber. (b) Critical position x_c, determined by the normalized gain k and injected power ratio γ. The critical positions divide the fiber into two parts, with and without the spectral hole burning phenomenon.

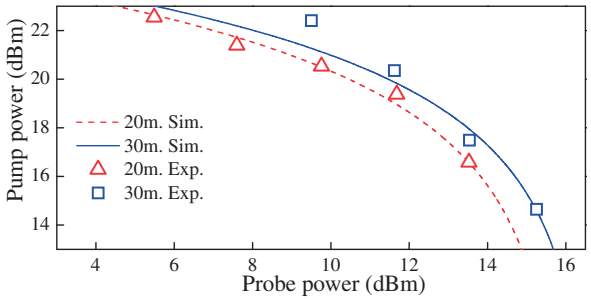

Fig. 3. Critical powers for two different positions in a 50-m-long fiber. Solid and dashed curves: simulation; open symbols: experiment.

of the critical powers is essentially the same as that of the critical position. They can be determined by the contour (i.e., k–γ curve) at a fixed position x in Fig. 2(b), and then deduced by

$$P_s(0) = k/GL,$$
$$P_p(L) = \gamma k/GL. \tag{5}$$

As an example, the calculated critical powers for two positions ($z = 20$ or 30 m) of a 50-m-long fiber are depicted in Fig. 3. It is clear that the higher z positions require greater critical powers. This is because the pump depletion is weaker and the distortion of the BGS is less severe if the position is much closer to the fiber's far end.

The experimental setup used to confirm the theoretical analysis is depicted in Fig. 4. Lightwave generated by a 1552 nm distributed-feedback laser diode (DFB-LD) is divided into two parts. One part, used as the pump wave, is launched into a circulator and is then injected into the fiber under test (FUT), which is composed of two segments (20 m plus 30 m)

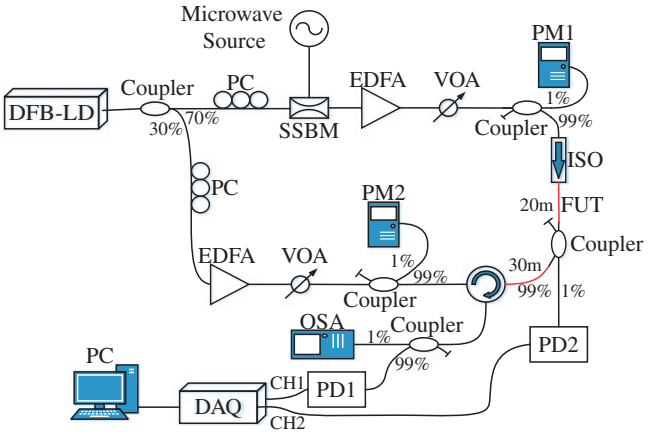

Fig. 4. Experimental setup. DFB-LD: distributed-feedback laser diode, PC: polarization controller, SSBM: single side-band modulator, EDFA: erbium-doped fiber amplifier, VOA: variable optic attenuator, PM: power meter, ISO: isolator, FUT: fiber under test, PD: photo-detector, OSA: optical spectrum analyzer, and DAQ: data acquisition.

of a dispersion compensating fiber (DCF). A polarization controller (PC) adjusts the polarization states to guarantee the optimal Brillouin gain. The frequency of the other part, serving as the probe wave, is down-shifted by a single side-band modulator (SSBM), which is driven by a microwave source.

To detect the BGS in the middle of the FUT, one 1:99 coupler is inserted between the two segments. The BGS at the end of the FUT is detected by a photo-diode (PD1) positioned after the circulator. The 1% port is detected by another photo-diode (PD2) to measure the amplified probe in the middle of the FUT. The optical spectrum after the SSBM is illustrated in Fig. 5(a), which shows that the carrier and the upper side-band are suppressed by 30 dB through properly adjusting the bias. The pump–probe frequency offset is detuned by a microwave source around 9.66 GHz (Brillouin frequency shift of the DCF at 1550 nm). During the detuning of the probe wave, its power can fluctuate more or less. To remove this effect, we utilize a differential measurement by recording the signals twice when the pump wave is turned on or off. In this way, the BGS can be effectively extracted from the background noise through a simple subtraction. An example is described in Fig. 5(b), where the signals of the differential measurement and the extracted BGS (even higher-order peaks) are clearly shown. A data acquisition (DAQ) card and a computer record the BGS signals both in the middle and the end of the FUT. It must be noted that two sets of erbium-doped fiber amplifiers (EDFA) and variable optic attenuators (VOA) are used in the two parts to guarantee the application of suitable optical power in the FUT. Two power meters (PM1, PM2), following two 1:99 couplers, are employed to monitor the probe and pump power, respectively.

Figure 6 summarizes the obtained BGS under different pump powers and at different positions of the 50-m-long fiber, which is in a qualitative accordance with the theoretical result in Fig. 2(a). The probe power is fixed at 9.8 dBm. At the far end [see Fig. 6(a)], the BGS rises with increasing power and always preserves the Lorentz shape. However, in the middle of the fiber [see Figs. 6(b) and 6(c)], the Brillouin

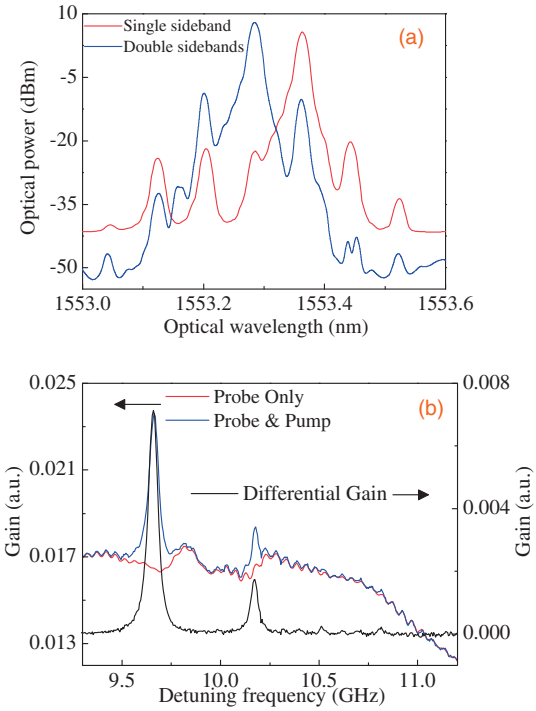

Fig. 5. (a) Optical spectra modulated by the SSBM. (b) Brillouin gain signals before and after the differential measurement.

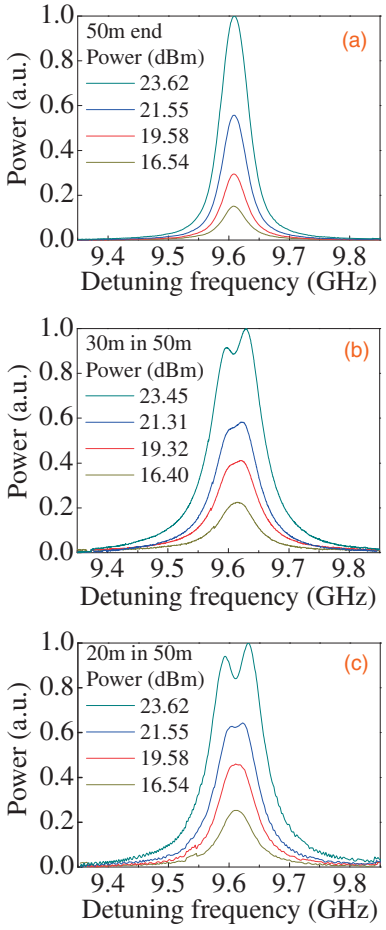

Fig. 6. Brillouin gain signals acquired under different pump powers at different positions. (a) Fiber end, (b) $z = 30$ m, and (c) $z = 20$ m.

gain keeps rising with the increase of optical power, while the peak at the local Brillouin frequency shift seems to be gradually saturated and a hollow starts appearing when it reaches ~20 dBm, which is indicative of the spectral hole burning phenomenon. The hollow in the BGS may introduce large errors to pump–probe-based Brillouin distributed sensors[10–12] because it disables the peak-searching capability of the Brillouin frequency shift. It is also worth noting that the two peaks around the hollow are slightly asymmetric. This could be attributed to the fact that the electrical amplifier for the microwave source has a slightly non-uniform response around 9.6 GHz and/or that the polarization states along the fiber change during the measurement. A future investigation has been planned to clarify the cause of this feature. The pump power leading to BGS saturation is approximately characterized as the critical pump power, which is 21.3 dBm at $z = 30$ m or 19.6 dBm at $z = 20$ m. Note that the exact situation of the BGS saturation is hardly confirmed since it is very sensitive to the pump and probe powers. The critical pump powers approximately measured for several probe powers are illustrated by open symbols in Fig. 3. It shows that the experimental observation matches well the theoretical analysis (see solid curves in Fig. 3).

In summary, we have theoretically and experimentally studied the spectrum distortion phenomena induced by pump depletion of stimulated Brillouin scattering in a pump–probe-based configuration. Broadening, saturation, and spectral hole burning are observed under different powers and/or at different positions in the fiber. Among those, the spectrum saturation defines the critical conditions (power and position) that physically characterize these phenomena. This new finding of spectrum distortion may be advantageous for developing high-performance Brillouin-based distributed fiber-optic sensors[9–12] and very useful for application to programmable optical filtering.[14]

Acknowledgments This work was partially supported by the National Natural Science Foundation of China (Grant Nos. 61007052 and 61127016), International Cooperation Project from the Ministry of Science and Technology of China (Grant No. 2011FDA11780), SRFDP of MOE (Grant No. 20130073130005), Shanghai Pujiang Program (Grant No. 12PJ1405600), Shanghai Excellent Academic Leader Program (Grant No. 12XD1406400), and the State Key Lab Project of Shanghai Jiao Tong University (2014ZZ03016).

1) G. P. Agrawal, *Nonlinear Fiber Optics* (Academic Press, New York, 2007) 4th ed.
2) E. P. Ippen and R. H. Stolen, Appl. Phys. Lett. **21**, 539 (1972).
3) V. I. Kovalev and R. G. Harrison, Phys. Rev. Lett. **85**, 1879 (2000).
4) Y. Takushima and K. Kikuchi, Opt. Lett. **20**, 34 (1995).
5) L. Stépien, S. Randoux, and J. Zemmouri, Phys. Rev. A **65**, 053812 (2002).
6) Y. Mizuno and K. Nakamura, Appl. Phys. Lett. **97**, 021103 (2010).
7) A. Kobyakov, S. Darmanyan, M. Sauer, and D. Chowdhury, Opt. Lett. **31**, 1960 (2006).
8) V. I. Kovalev and R. G. Harrison, Opt. Express **15**, 17625 (2007).
9) W. Zou, Z. He, and K. Hotate, Opt. Express **17**, 1248 (2009).
10) X. Bao and L. Chen, Sensors **11**, 4152 (2011).
11) L. Thévenaz, S. F. Mafang, and J. Lin, Opt. Express **21**, 14017 (2013).
12) W. Li, X. Bao, Y. Li, and L. Chen, Opt. Express **16**, 21616 (2008).
13) W. Zou, Z. He, and K. Hotate, Appl. Phys. Express **3**, 012501 (2010).
14) X. Fan, Z. He, Y. Mizuno, and K. Hotate, Opt. Express **13**, 5756 (2005).